Supplemental Material:
Consistent Shepard Interpolation for SPH-Based Fluid Animation

STEFAN REINHARDT, University of Stuttgart, Hochschule der Medien, Germany
TIM KRAKE, University of Stuttgart, Hochschule der Medien, Germany
BERNHARD EBERHARDT, Hochschule der Medien, Germany
DANIEL WEISKOPF, University of Stuttgart, Germany

1 OVERVIEW

In our paper, we present a technique to reduce errors induced by the discretization process. In this document, we provide additional information for the presented examples. As mentioned in the paper, we test our method in combination with weakly compressible smoothed particle hydrodynamics (WCSPH) [Becker and Teschner 2007] and divergence free smoothed particle hydrodynamics (DFSPH) [Bender and Koschier 2017]. We compare our method with classical Shepard correction [Shepard 1968] and simulations without kernel correction.

In Section 2, we provide additional renderings to the fluid block scenario for WCSPH (Figure 3) and DFSPH (Figure 4). In Figure 5, the mean and max local density variance for both WCSPH and DFSPH are plotted. Similar information is provided for the fluid pillar scenario in Section 3 as well as for the corner dam break scenario (Section 4). For the corner dam break scenario, we additionally provide renderings, where the particles are color-coded by their local density variance. In Section 5, selected renderings of the fountain scenario conducted with DFSPH are given.

Figure 1. Linear color map used in the examples throughout this document. The unit and value range will be specified in the specific example.

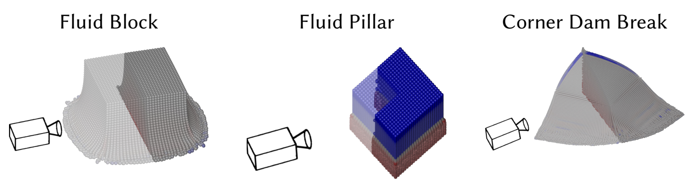

Figure 2. Pictograms of the test cases to understand the orientation of the camera in the scene.

2 FLUID BLOCK

2.1 WCSPH

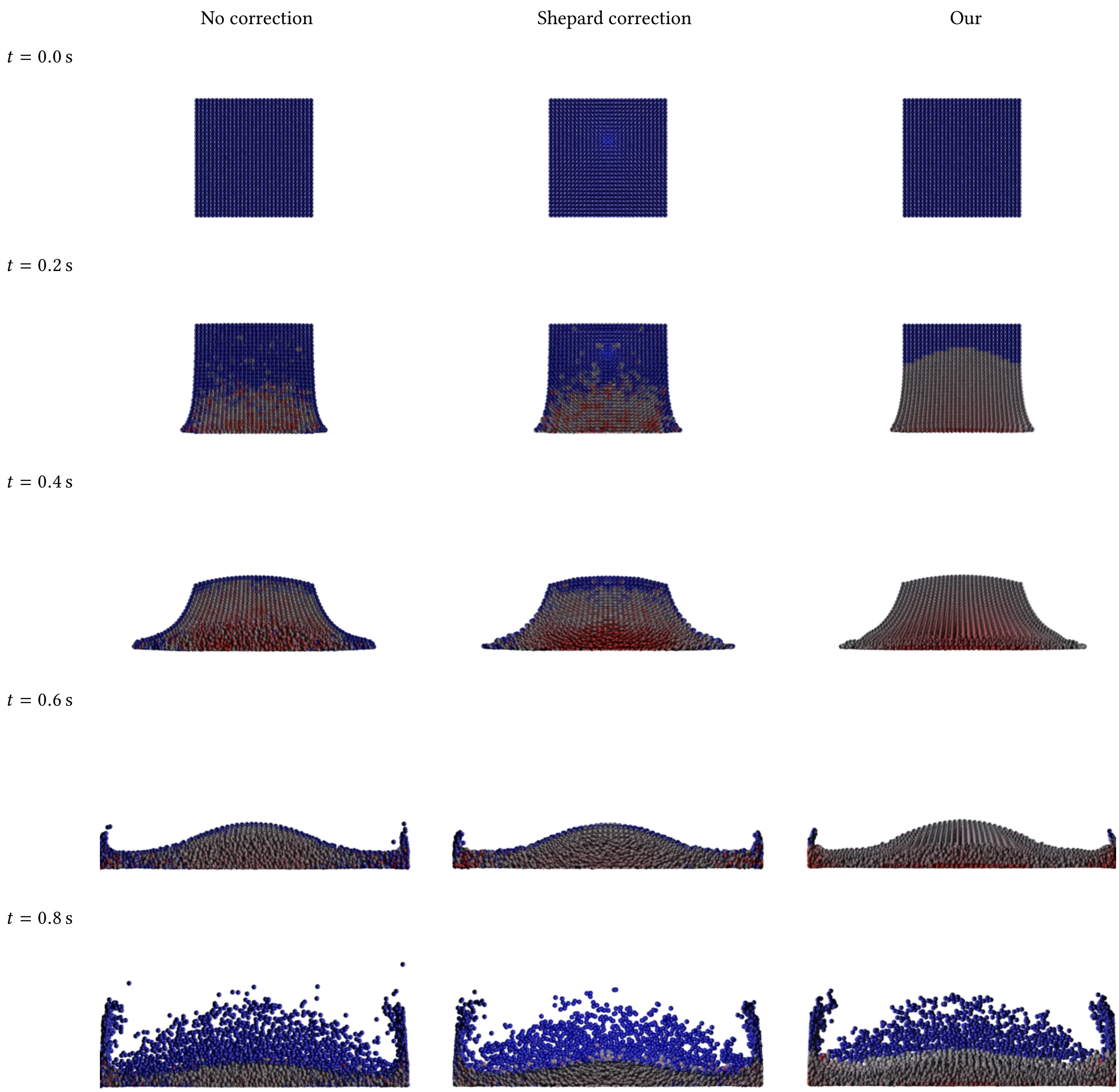

Figure 3. Selected renderings from the fluid block scenario simulated with WCSPH. From left to right: Simulations without any kernel correction, with Shepard kernel, and with our method. Particles are colored with respect to density, where the lowest value (blue) corresponds to $997.5\,\frac{\text{kg}}{\text{m}^3}$ and the highest value (red) to $1002.5\,\frac{\text{kg}}{\text{m}^3}$. We observe that we significantly improve the smoothness of the density field. Especially at time $t = 0.2$ s, it is noticeable that with our method one smooth wave front appears (second row, right), whereas the other two simulations result in a noisy density field.

2.2 DFSPH

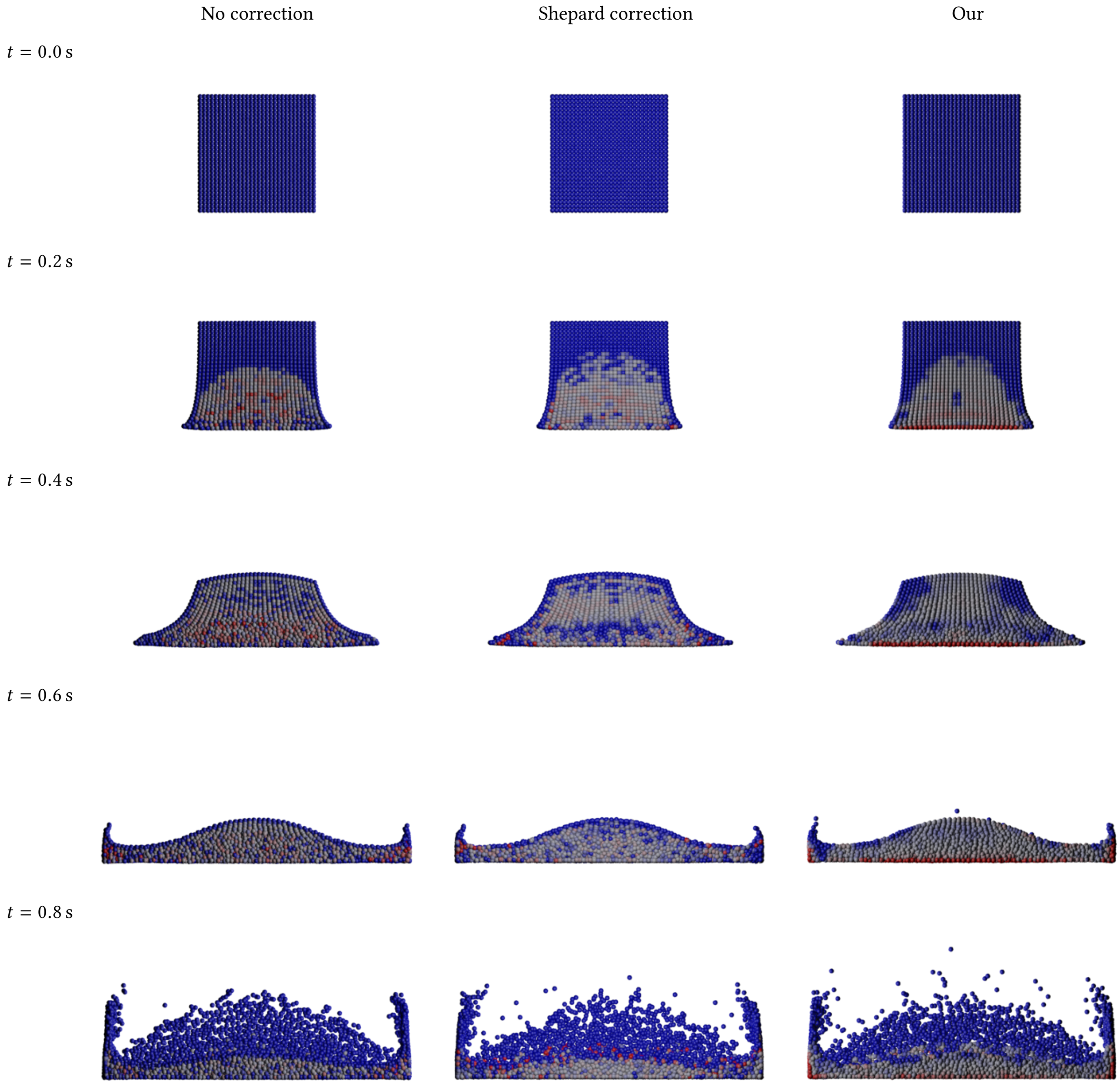

Figure 4. Side-by-side comparison of the different methods in the fluid block scenario simulated with DFSPH. From left to right: Simulation conducted without any kernel correction, with Shepard kernel and with our method. Similar to Figure 3, particles are colored with respect to density. The lowest value (blue) again corresponds to $997.5\,\frac{\mathrm{kg}}{\mathrm{m}^3}$ and the highest value (red) to $1002.5\,\frac{\mathrm{kg}}{\mathrm{m}^3}$. We recognize that the improvements are less significant when using our method, but in comparison to the other methods, we still achieve a smoother density field.

2.3 Quantitative Evaluation

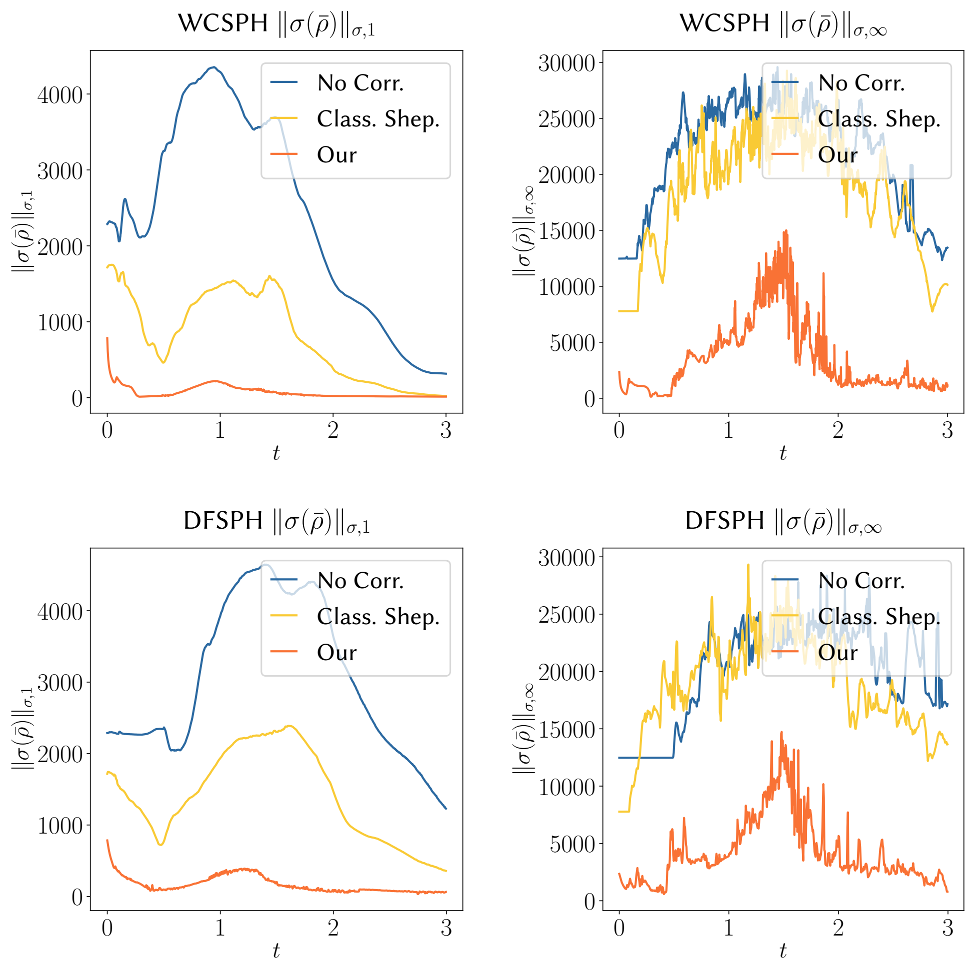

Figure 5. Density variance measurements of the fluid block scenario. The norm $\|\sigma(\bar{\rho})\|_{\sigma,1}$ representing the mean density variance is shown on the left and the max norm $\|\sigma(\bar{\rho})\|_{\sigma,\infty}$ on the right. In the upper row, the measurements of simulations with WCSPH are shown, and in the lower row, the ones with DFSPH. Lower density variance corresponds to a smoother density distribution. In all cases, we observe that we significantly improve the smoothness of the density field. Considering the maximum density variance, we observe that the local density variance is even increased at some points in time when employing classical Shepard correction. This could be interpreted that the classical Shepard correction introduces noise at some points in space and time.

3 FLUID PILLAR

3.1 WCSPH and DFSPH

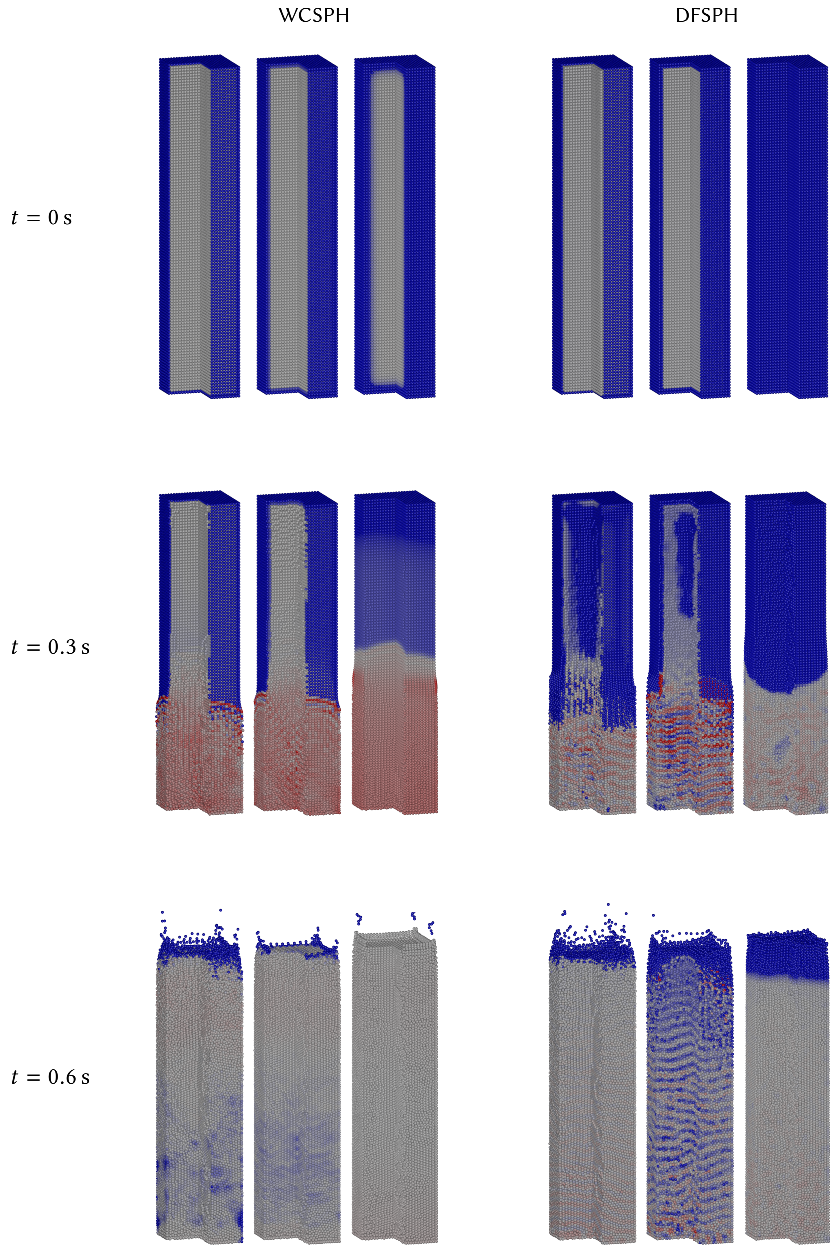

Figure 6. Selected snapshots from the fluid pillar scenario conducted with WCSPH and DFSPH. Simulations without kernel corrections (left), with classical Shepard correction (middle), and with our correction (right) are shown. The particles are color-coded with respect to density: the lowest value (blue) is set to $998\,\frac{\mathrm{kg}}{\mathrm{m}^3}$ and the highest value (red) to $1002\,\frac{\mathrm{kg}}{\mathrm{m}^3}$ for DFSPH (right column). For the simulations with WCSPH, the value range is adjusted so the lowest value corresponds to $970\,\frac{\mathrm{kg}}{\mathrm{m}^3}$ and the highest to $1030\,\frac{\mathrm{kg}}{\mathrm{m}^3}$. We again observe the same behavior as in the fluid block scenario (see Figure 3 and Figure 4). In this case, classical Shepard kernel induces a coarse-scale noise in the density field for both kind of simulations (second row left and right as well as third row on the right).

3.2 Quantitative Evaluation

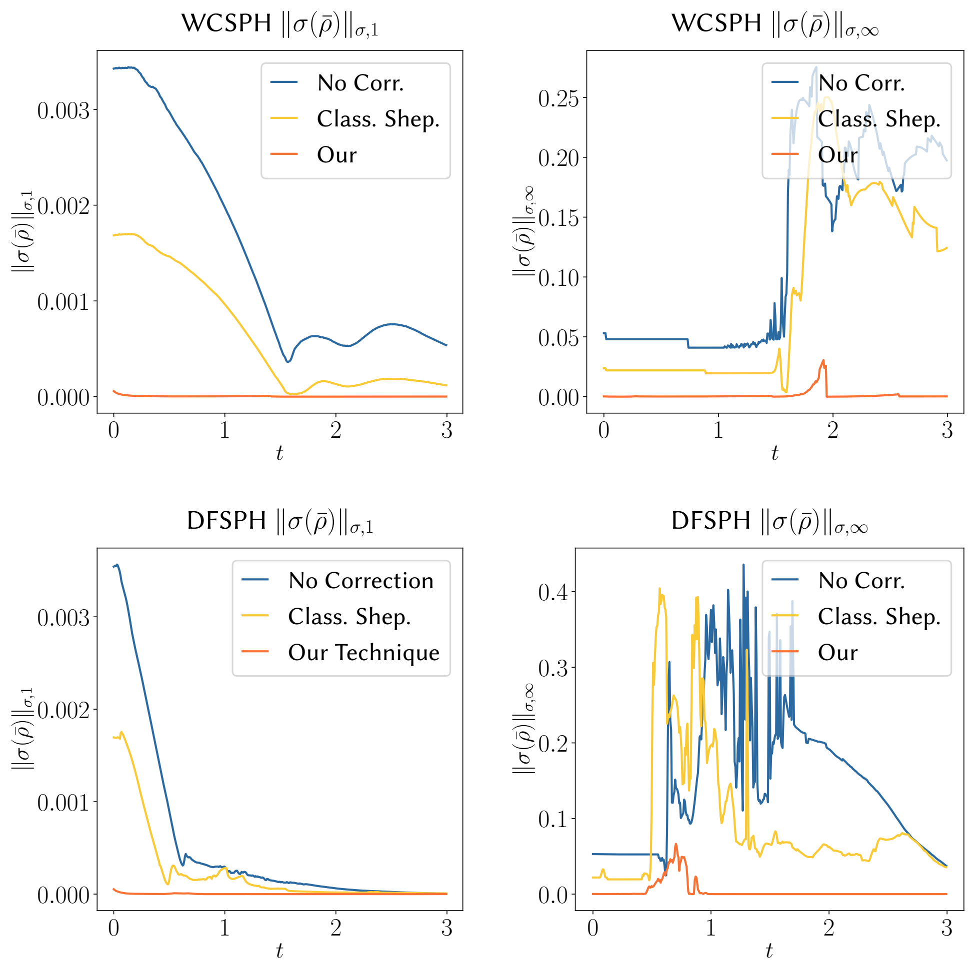

Figure 7. Density variance measurements of the fluid block scenario. Similar to Figure 5, the mean norm $\|\sigma(\bar{\rho})\|_{\sigma,1}$ is shown on the left and the max norm $\|\sigma(\bar{\rho})\|_{\sigma,\infty}$ on the right. The diagrams in the upper row contain the measurements of simulations conducted with WCSPH and the lower row the ones with DFSPH. We again observe the same overall behavior. Additionally, we recognize an interesting effect: when the fluid is repelled after the moment of highest compression (at $t \approx 1.75$ s for WCSPH and $t \approx 0.75$ s for DFSPH), the mean density variance increases for uncorrected and classical Shepard correction, whereas it does not with our method. Considering the maximum density variance, this effect is even more significant.

4 CORNER DAM BREAK

4.1 WCSPH

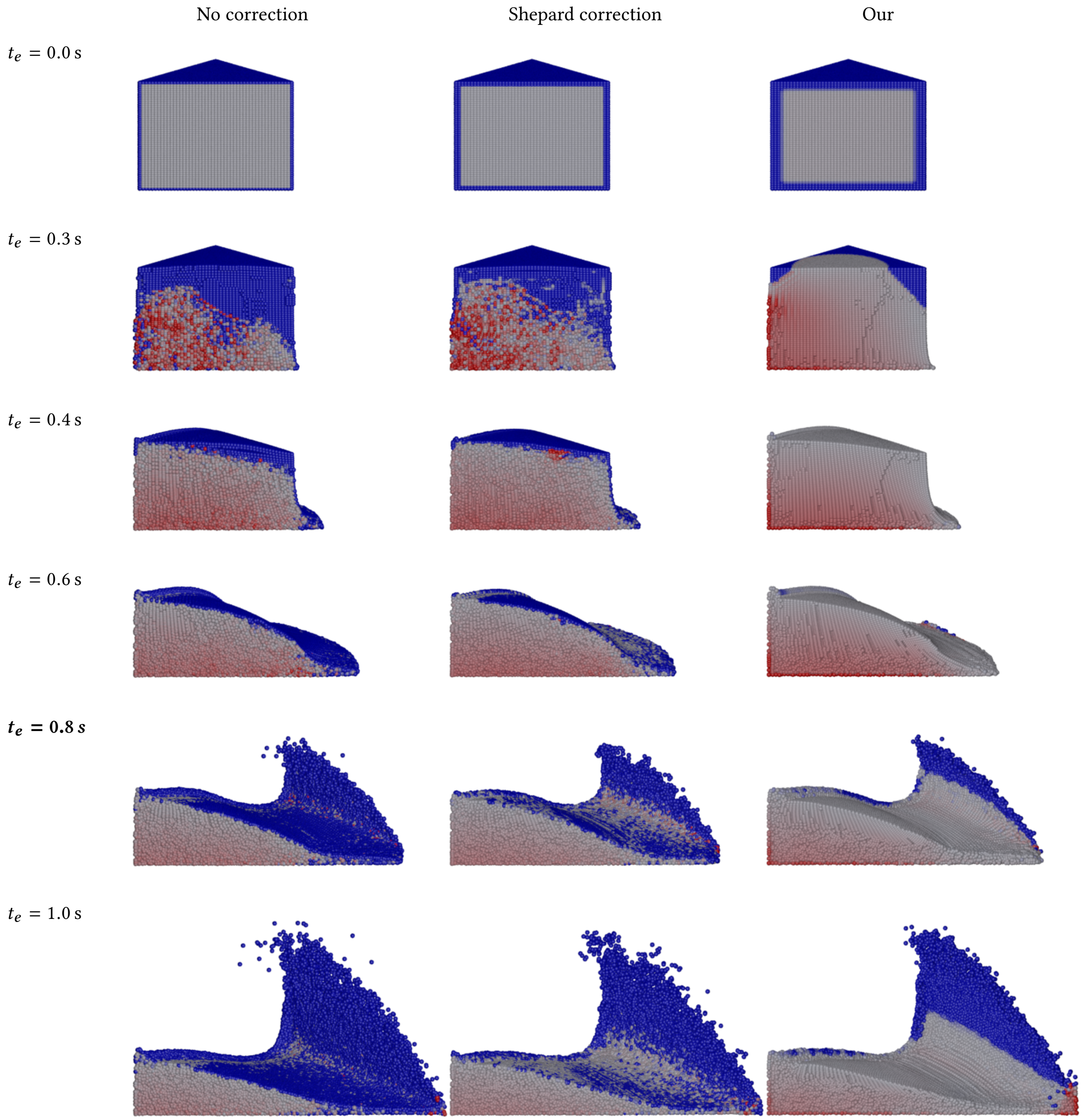

Figure 8. Selected renderings of the corner dam break scenario with WCSPH. From left to right: no kernel correction, Shepard correction, and ours. The particles are color-coded with respect to density, where the lowest value (blue) corresponds to $997\,\frac{\mathrm{kg}}{\mathrm{m}^3}$ and the highest value (red) to $1003\,\frac{\mathrm{kg}}{\mathrm{m}^3}$. To look into the fluid body, a plane is placed diagonal through the simulation domain and the particles on one side of it are hidden. Again, the same behavior is observed. Additionally, we recognize that less splashes of single particles occur (second last and last row) when using our method.

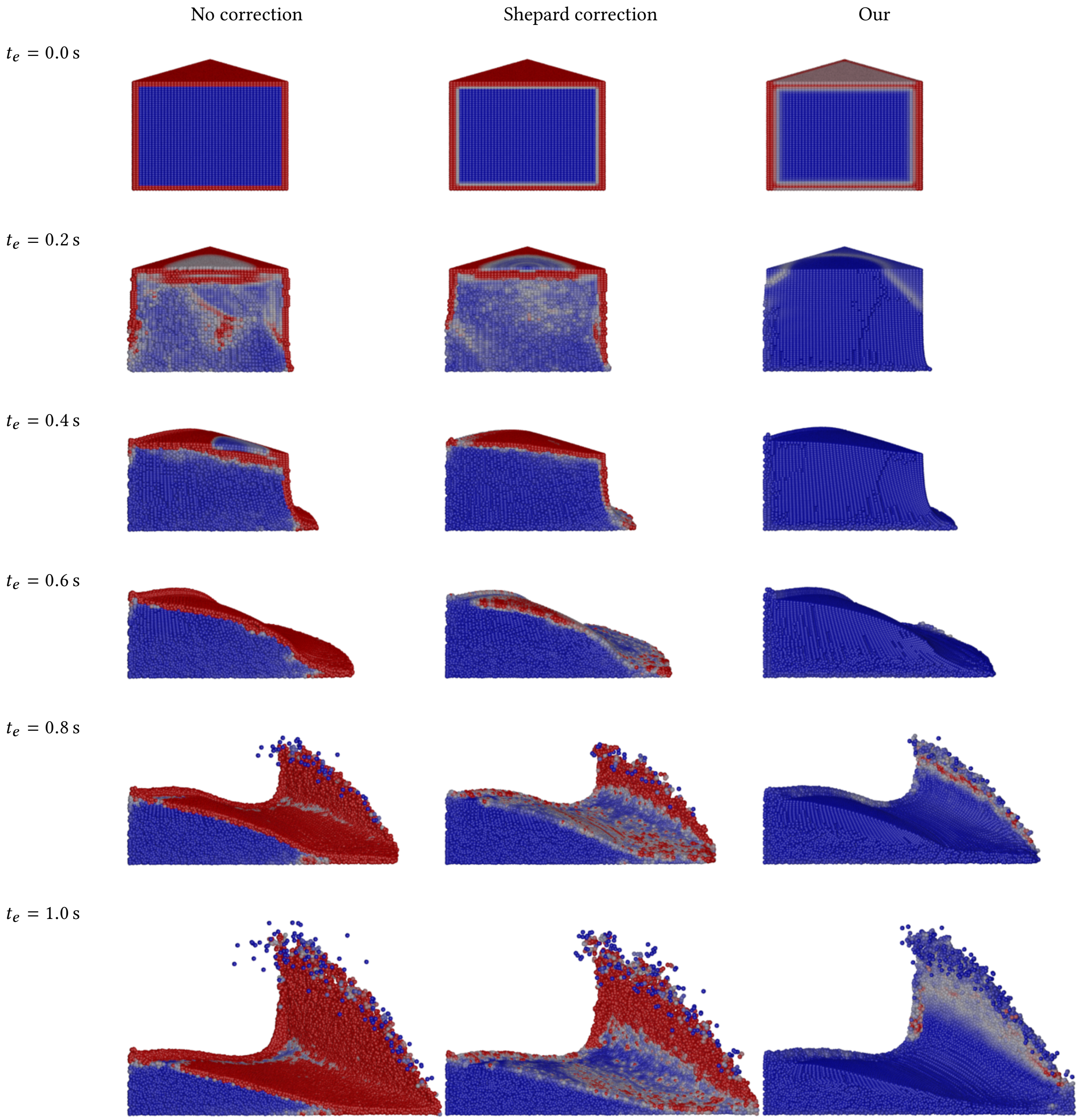

Figure 9. Selected renderings of the corner dam break scenario with WCSPH. From left to right: no kernel correction, Shepard correction, and ours. The particles are color-coded with respect to local density variance, where the lowest value (blue) corresponds to 0 and the highest value (red) to 3000. Again, it can be observed that using our method the noise in the density field is reduced, which is equivalent to reducing the local density variance. The cut through the fluid shows that we do not only improve the smoothness of the density field at the surface but also beneath.

4.2 DFSPH

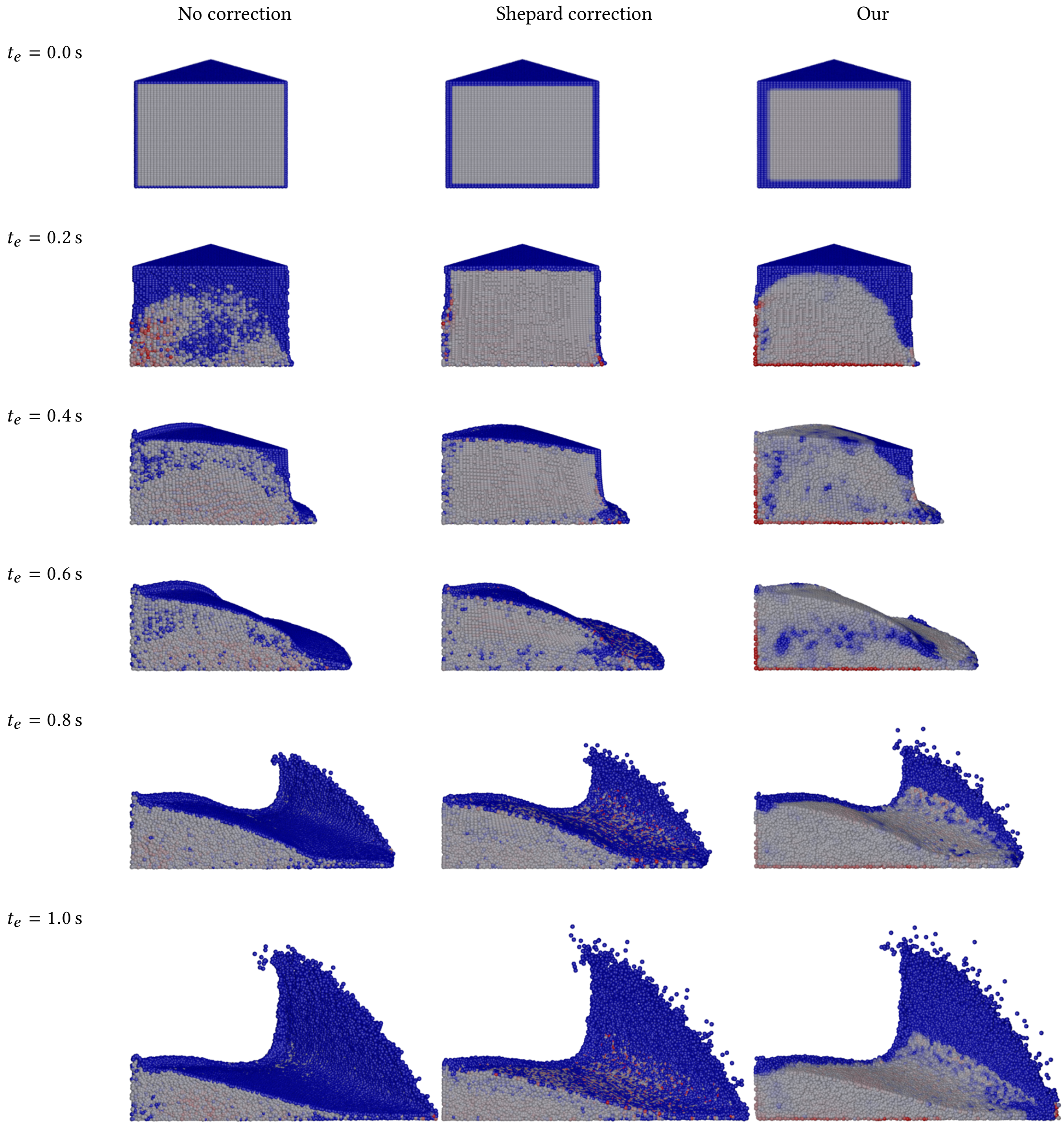

Figure 10. Selected renderings of the corner dam break scenario conducted with DFSPH. From left to right: no kernel correction, Shepard correction, and ours. The particles are color-coded with respect to density, where the lowest value (blue) corresponds to $997 \frac{\mathrm{kg}}{\mathrm{m}^3}$ and the highest value (red) to $1003 \frac{\mathrm{kg}}{\mathrm{m}^3}$. Even when simulating with DFSPH, we observe some noise in the density field (left column). It can slightly be reduced by employing classical Shepard correction but some fine-scale density noise is still present (see, e.g., $t = 0.6$ s). Even though our method does not completely remove the noise in the density field as with WCSPH, it still improves the smoothness of the density field.

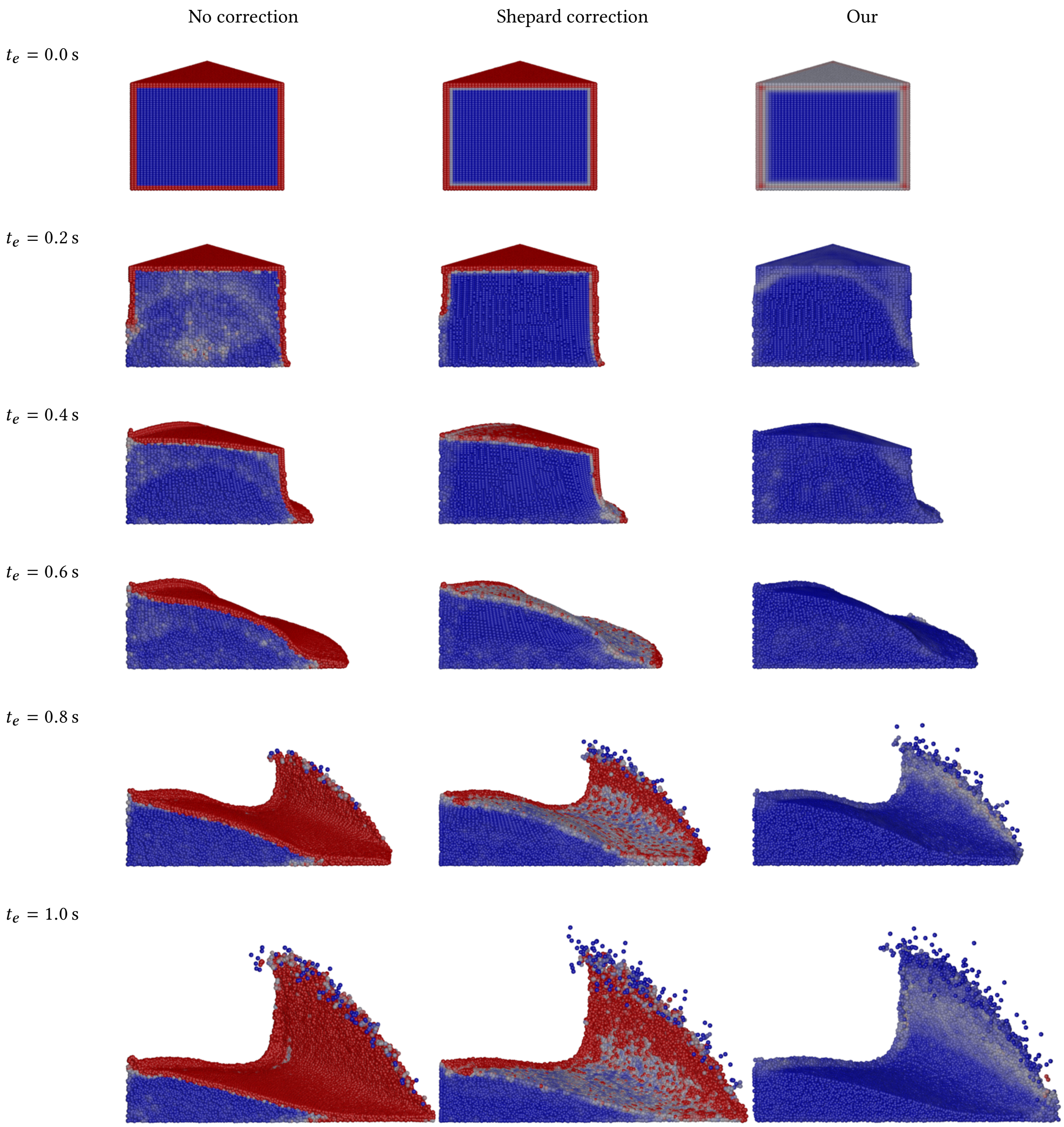

Figure 11. Selected renderings of the corner dam break scenario with WCSPH. From left to right: no kernel correction, Shepard correction, and ours. The particles are color-coded with respect to local density variance, where the lowest value (blue) corresponds to 0 and the highest value (red) to 3000. This shows that we still significantly improve the smoothness of the density field, as the local noise is removed almost completely.

4.3 Quantitative Measurements

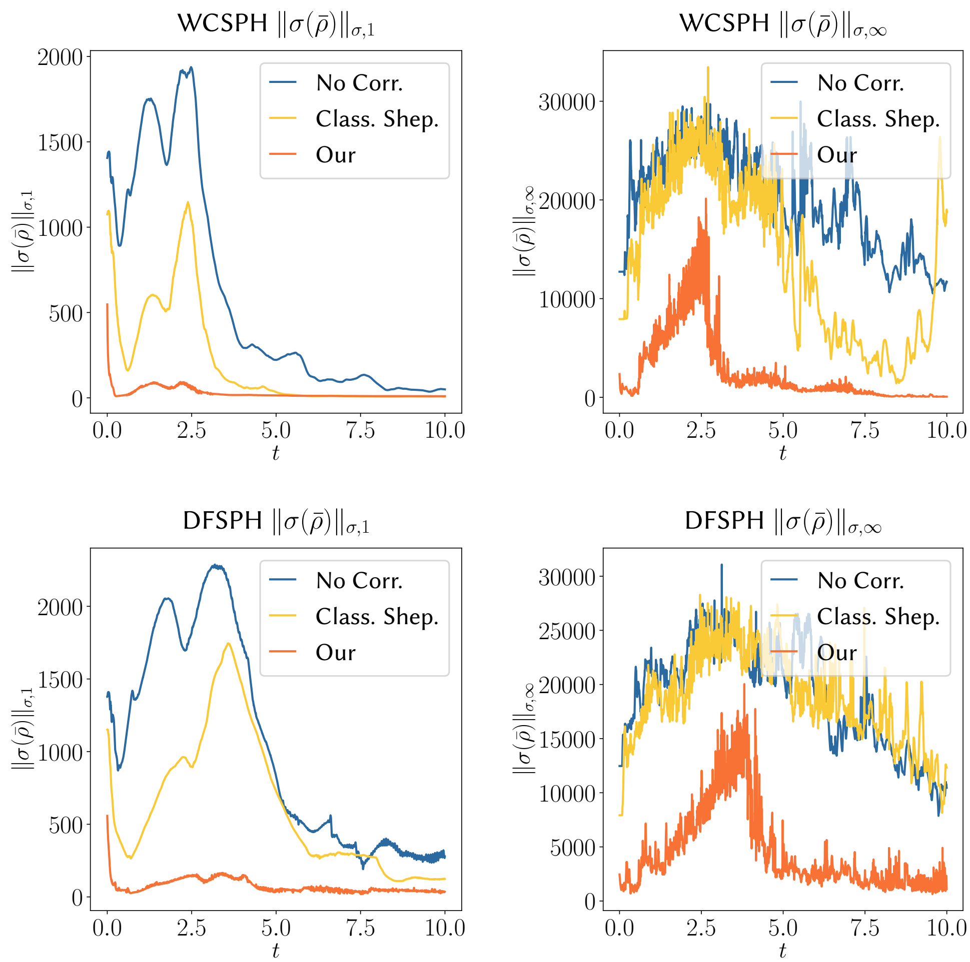

Figure 12. Density variance measurements of the corner dam break scenario to quantify the observations. Again, the norm $\|\sigma(\bar{\rho})\|_{\sigma,1}$ is shown on the left and the norm $\|\sigma(\bar{\rho})\|_{\sigma,\infty}$ on the right. The upper row contains the measurements of simulations conducted with WCSPH and the lower row the ones with DFSPH. We observe the same overall behavior as in the other scenarios.

5 FOUNTAIN

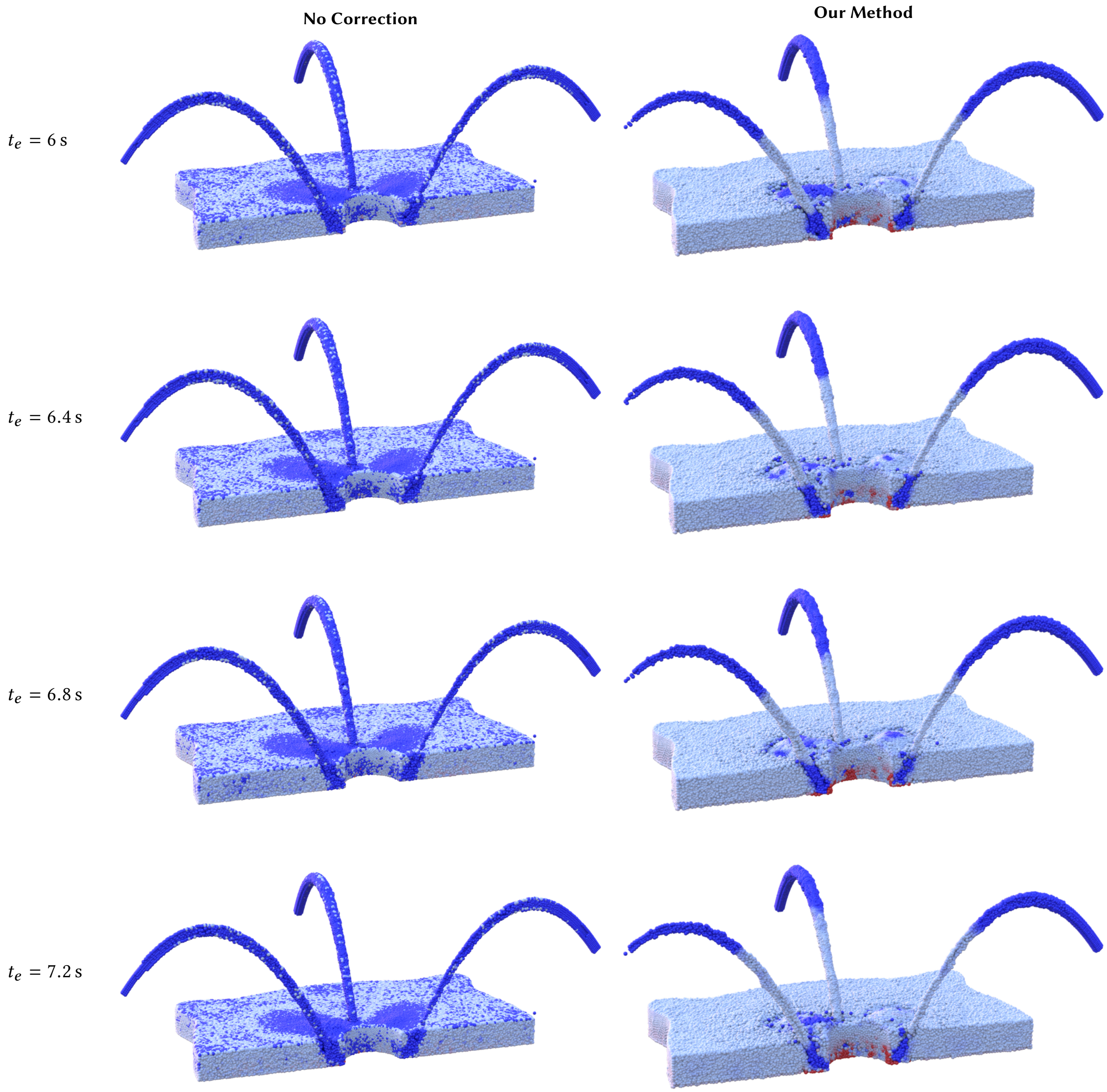

Figure 13. Selected renderings of the fountain scenario with DFSPH. Particles are again color coded with respect to density, where the lowest value (blue) corresponds to 995 $\frac{\mathrm{kg}}{\mathrm{m}^3}$ and the highest (red) to 1005 $\frac{\mathrm{kg}}{\mathrm{m}^3}$. Again, we obtain a smooth density field. This example is used to perform a stress test for our algorithm with regard to convergence of the power method. Particles are continuously added and initialized with $c_i = 1$. This could affect the convergence of our algorithm as the temporal coherence of the correction factors is destroyed. We observe that our algorithm is very robust and only needed on average 2.12 iterations and never more than 4.

5.1 Quantitative Measurements

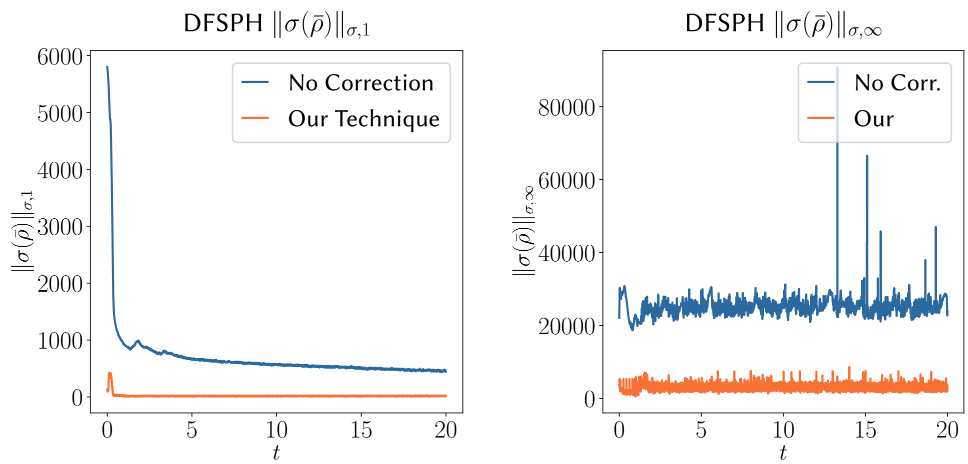

Figure 14. Measurements of the mean and max local density variance of the fountain scenario.

6 SCALING OF THE STIFFNESS CONSTANT

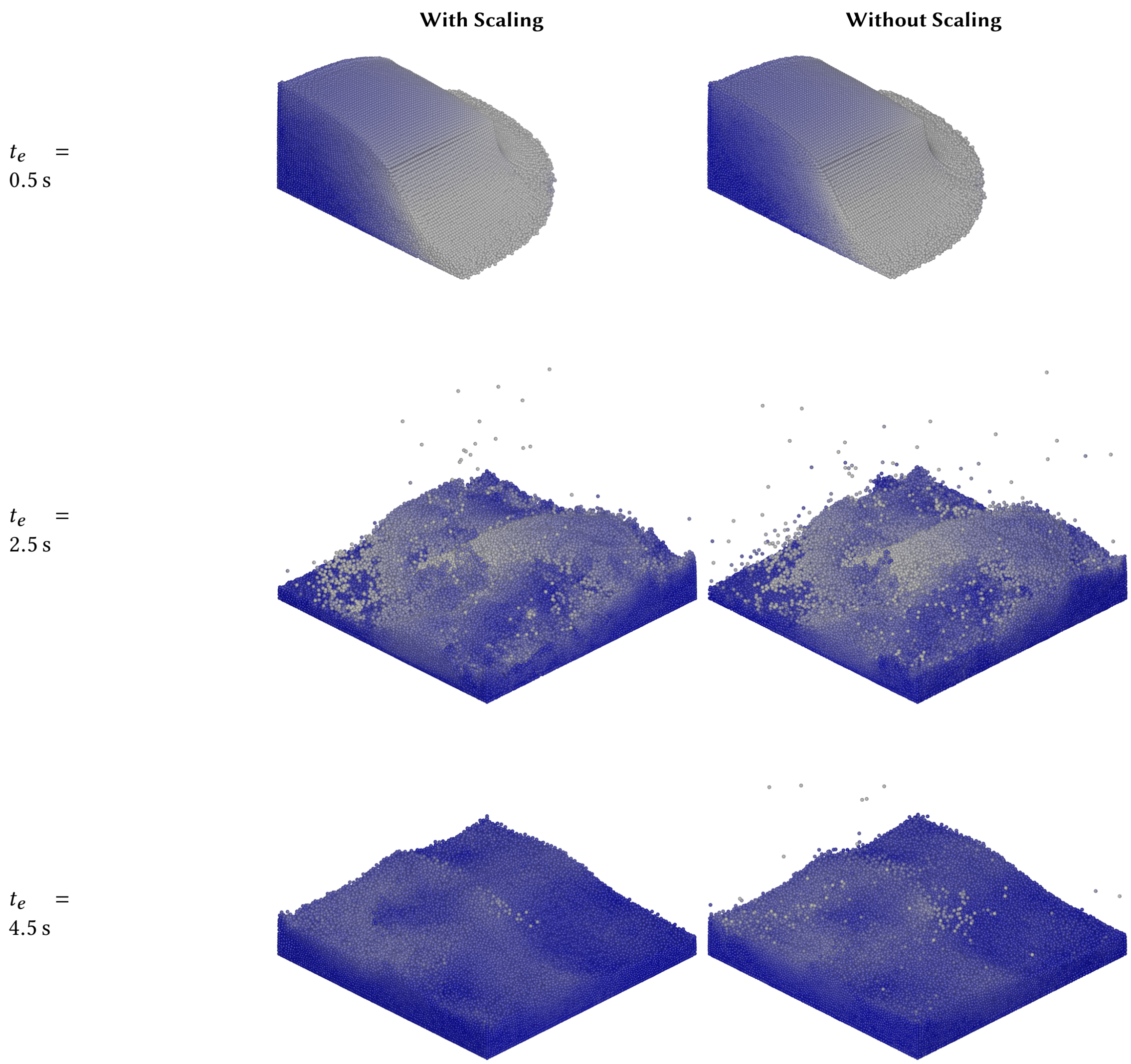

Figure 15. Selected renderings of the corner dam break scenario. The fluid was simulated with DFSPH and our correction method. In the left column, renderings of the simulation with scaling of the stiffness constant κ_i are shown. In the right one without scaling. We observe decreased amount of splashes at $t_e = 2.5$ s and a bit a smoother surface at $t_e = 4.5$ s when scaling the stiffness constant.

REFERENCES

M. Becker and M. Teschner. 2007. Weakly compressible SPH for free surface flows. In *Eurographics/SIGGRAPH Symposium on Computer Animation*. 209–218. https://doi.org/10.2312/SCA/SCA07/209-218

J. Bender and D. Koschier. 2017. Divergence-free SPH for incompressible and viscous fluids. *IEEE Transactions on Visualization and Computer Graphics* 23, 3 (2017), 1193–1206. https://doi.org/10.1109/TVCG.2016.2578335

D. Shepard. 1968. A two-dimensional interpolation function for irregularly-spaced data. In *Proceedings of the 1968 23rd ACM National Conference*. 517–524. https://doi.org/10.1145/800186.810616